JOURNAL OF AIRCRAFT
Vol. 33, No. 1, January–February 1996

Aeroelastic Model Design Using Parameter Identification

Mark French*
U.S. Air Force Wright Laboratory, Wright–Patterson Air Force Base, Ohio 45433
and
F. E. Eastep†
University of Dayton, Dayton, Ohio 45469

Wind-tunnel model design can be very involved, so an approach has been developed that uses optimization methods to automate it. The model design process has been divided into separate stiffness design and mass design stages. Then, a sample structure was manufactured and subjected to static and modal testing using laser holographic techniques. The predicted flutter response of the model matches the predicted flutter response of the full-scale wing very closely.

Nomenclature

c = element of calculated flexibility matrix
F = objective function
g = constraint
K = stiffness matrix
k = proportionality constant
M = mass matrix
m = total mass
x = element of eigenvector matrix
δ = element of target flexibility matrix
ω = natural frequency

Introduction

TESTING aeroelastically scaled wind-tunnel models is a common task in flight vehicle development programs. The object of the testing is often to verify the numerically predicted aeroelastic characteristics of an entire vehicle or some component of it. In some tests, the goal is simply to verify analytical methods. Then, the model must only represent the full-scale vehicle in a qualitative sense. Quite often, though, the scaled model is intended to exactly model the response of the full-scale structure.[1] This is the most general form of the aeroelastic model design problem and it is the one addressed here.

A method has been developed that uses a numerical optimization approach to design an aeroelastically scaled wind-tunnel model. Previous efforts[2,3] have been aimed at demonstrating feasibility of the basic idea and were limited to the stiffness design of the model. This work has been refined and extended to include selection of tuning masses.

An aeroelastically scaled model is one for which static deflection and modal behavior are related to that of a full size article by simple scaling rules.[4] The model designer must produce a structure that matches predetermined mass and stiffness properties. There is little published work dealing directly with aeroelastically scaled model design. However, the problem may be treated as a parameter identification problem.

Requirements for a good parameter identification method were laid out by Ibrahim and Saafan.[5] An assessment of the capabilities of parameter identification was presented by Berman.[6] These references suggest requirements for a usable method: 1) the ability to handle general structures, 2) no need for complete response information, and 3) no need for accurate initial guess at correct design.

Background

A classical form of the parameter identification problem involves determining the coefficients of a system of linear equations. The identification process is based on some system response measurement that is assumed to be a solution of the equations of the mathematical representation.[7]

A large subset of the literature dealing with the parameter identification problems deals with model update or model improvement methods. These methods use some approximation to the desired system as the starting point for a procedure that uses system output to improve the accuracy of the initial model. A successful class of methods uses optimization methods to correct the mathematical representation of structures.[8–11] A concise method unifying this approach was presented by Berman and Nagy.[12]

Many methods intended to isolate errors in finite element models have been proposed,[13–15] all of which operate directly or indirectly on physical parameters. Wei and Janter[16] suggest operating directly on parameters of a finite element model. This basic approach has been expanded with more recent work being presented by Ewing and Venkayya[17] and Ewing and Kolonay.[18] A preliminary effort at including system identification capabilities in a general purpose finite element code is presented by Gibson.[19]

The method presented here uses constrained numerical optimization methods to modify a finite element representation of the model structure so that some measure of the difference between the calculated and desired responses is minimized. By operating directly on the finite element model, orthogonality of calculated eigenvectors, symmetry of system matrices, and validity of individual system matrices is assured. Also, the result of the design process is information that can be used to fabricate a model with no postprocessing.

The process presented here is broken down into two steps. In the first step, optimization methods are used to size the structure for stiffness only. The element sizes are then fixed and concentrated masses are added to the structure to give the desired modal response. The sizes of the masses are determined using a second optimization-based method.

Stiffness Design

Wind-tunnel model design is fundamentally different than design of a full-scale structure. The designer of a flight vehicle

Received Feb. 22, 1994; revision received June 21, 1995; accepted for publication June 29, 1995.

*Aerospace Engineer, Flight Dynamics Directorate; currently Development Engineer, Lear Seating Corporation, Advanced Technology and Test Center, Southfield, MI 48034. Member AIAA.

†Professor of Aerospace Engineering. Associate Fellow AIAA.

must satisfy strength, weight, performance, and stability criteria and may accept any resulting stiffness properties. The wind-tunnel model designer must design a structure that has a predetermined set of stiffness and mass properties. We assume for this work that the known stiffness properties come from a finite element model of the full-scale structure, though perhaps one which has been tuned to agree with test results.

The approach for the stiffness design task is to create an error function based on the difference between calculated and desired displacements due to a group of specified unit loads and use an optimization routine to change the design so that function is minimized. When using a finite element representation of some structure, the vector of displacements due to a unit load in a single degree of freedom j is the jth column of the flexibility matrix.

In the ideal case, the final error function value would be zero. Then, the calculated flexibility matrix of the wind-tunnel model structure would match the desired one scaled from the full-size structure. Ideally, displacements at all grid points would be specified using unit loads applied at all grid points. However, this can result in an unwieldy and possibly overconstrained problem. Thus, only selected elements are used in forming the objective function.

The input data consisted of grid point locations and element connectivity for the finite element representation and displacement data for a selected group of grid points. All stiffness design runs started with the same initial design. Automated design synthesis (ADS)[20] was used for all optimization tasks, except one routine provided by the developers of the method.[21]

The most effective approach used an interior penalty function method to minimize the objective function

$$F = \sum_{i=1}^{m} \sum_{j=1}^{n} k(\delta_{ij} - c_{ij})^2 \tag{1}$$

where δ_{ij} is the ijth term of the desired flexibility matrix and c_{ij} is the ijth term of the flexibility matrix calculated for the current design. The number of grid points for which displacements are specified is m and n is the number of columns of the flexibility matrix for which displacements are specified. An arbitrary constant is k and m and n will not, in general, be identical.

We also applied constraints of the form

$$g = (\delta_{ij} - c_{ij})^2 \leq 0 \tag{2}$$

Using the square of the displacement differences to form constraints means that the feasible region is a single point. Thus, the optimizer is searching for a point in design space at which all constraints intersect. There is no good way of being sure such a point even exists. In such a case, the object is to find a point in design space that is acceptably close to all of the constraints.

Mass Design

We considered two different approaches for the mass design. Both methods assumed that the stiffness design was complete and that an acceptable level of accuracy had been obtained. The first method minimized an error function based on natural frequencies. The assumption was that tuning masses to match natural frequencies on a structure that already had nominally correct stiffness characteristics would necessarily result in correct mode shapes. While perhaps correct in a theoretical sense, this approach performed poorly in practice. We found that accurate natural frequencies could be obtained for mass selections that poorly reproduced the desired mode shapes.

The more successful of the two methods used an interior penalty function to minimize an objective function based on the difference between desired and calculated mode shapes:

$$F = \sum_{i=1}^{m} \sum_{j=1}^{n} \left(\frac{\bar{x}_{ij} - x_{ij}}{\bar{x}_{ij}} \right)^2 \tag{3}$$

where x_{ij} is the ijth element of the eigenvector matrix whose columns are the eigenvectors of the structure. Overbars indicate the desired values. The term without overbars indicates the value calculated for the current design. The mode shape error function was normalized to make sure the function was not biased toward areas where the displacements are large. Getting proper node line locations is critical in matching flutter behavior. The normalizing process gives equal weight to small displacements near the node lines and large displacements at antinodes.

Constraints were formed using the difference between calculated and desired natural frequencies and a total mass constraint. Frequency constraints were of the form

$$g_i = [(\bar{\omega}_i - \omega_i)/\bar{\omega}_i]^2 \tag{4}$$

where, again, the overbar indicates the desired value and the term without overbars is the ith natural frequency of the current design. The total mass constraint is an equality constraint of the form

$$g = (\bar{m} - m)/\bar{m} = 0 \tag{5}$$

The total mass equality constraint was added to method two in order to force the design to the correct overall mass. Flutter may be considered as an energy transfer phenomenon. Kinetic energy in either the flow or the aircraft (depending on the reference frame chosen) is converted to kinetic and strain energy in the structure. Failing to properly scale the total mass of the structure would introduce unknown and potentially large differences between the kinetic energy of the model and that scaled from the full-scale structure. In such a situation, it would be unreasonable to expect aeroelastic properties to scale correctly.

Mass Design for Models with Skin

So far, the discussion has been limited to a description of structural design. The assumption has been that any structural elements other than the beam lattice and tuning weights may be ignored when calculating stiffness and mass. For situations in which this assumption is not valid, the mass and stiffness matrices for the complete model can be broken into separate components:

$$\begin{aligned} K_{\text{total}} &= K_{\text{frame}} + K_{\text{skin}} \\ M_{\text{total}} &= M_{\text{frame}} + M_{\text{tuning}} + M_{\text{skin}} \end{aligned} \tag{6}$$

The static equation of equilibrium is

$$[K_{\text{frame}} + K_{\text{skin}}]\{x\} = \{f\} \tag{7}$$

and the dynamic equation of equilibrium is

$$[K_{\text{frame}} + K_{\text{skin}}]\{x\} = \omega^2[M_{\text{frame}} + M_{\text{tuning}} + M_{\text{skin}}]\{x\} \tag{8}$$

The mass and stiffness matrices for the skin can be determined by any convenient means, though a finite element representation strongly suggests itself. At this point, there are two options. The first is to choose only parameters describing the frame as design variables, holding the structural properties of the skin constant. The second is to allow the properties of the skin to be used as design variables along with the frame.

Once the design variables are chosen, the design process continues as described earlier.

An initial guess for the tuning masses may be found by rewriting Eq. (8)

$$[K_{\text{frame}} + K_{\text{skin}}]\{x\} - \omega^2[M_{\text{frame}} + M_{\text{skin}}]\{x\} = \omega^2[M_{\text{tuning}}]\{x\} \tag{9}$$

If $[K_{\text{total}}]$ and $[M_{\text{total}}]$ are invertible, then

$$[M_{\text{tuning}}] = (1/\omega^2)[K_{\text{frame}} + K_{\text{skin}}] - [M_{\text{frame}} + M_{\text{skin}}] \tag{10}$$

A problem is that the tuning mass matrix calculated in Eq. (10) is not, in general, diagonal, and the tuning masses added to the structure modify only the diagonal terms of the mass matrix. One approach is simply to use the diagonal portion of the calculated tuning matrix as a starting point for the mass design of the model. Another approach is to modify the stiffness matrix using the nondiagonal terms of the calculated tuning matrix and repeat the stiffness design process.

Model Structure

One of the goals in designing this structure was to minimize fabrication costs, and so a simple all-metal structure was chosen. The structure was assumed to be made up of constant cross-sectional beam elements in a planar lattice. Test articles have been manufactured easily by machining the structure from a single plate of aluminum using a numerically controlled vertical end mill. Choosing this structure was not a reflection of any limitation of the method; it is valid for any structure that can be modeled using a finite element discretization.

In the stiffness design process, the heights of the elements were assigned and did not change. The widths of the elements were used as design variables. Typically, the beam heights were assigned at the maximum values that would allow the structure to fit inside the aerodynamic envelope of the wing. This was done to keep the structure as light as possible for a given stiffness distribution. Grid point locations for the finite element representation of the wind-tunnel model were fixed at the beginning of the design process and not used as design variables.

Sample Problem

A sample problem was developed to evaluate the design method. The wing is a clipped delta intended to simulate a common low AR fighter wing. The aerodynamic planform is presented in Fig. 1. The wing is assumed to be made of aluminum with 11 spars. The finite element model of the full-scale wing is presented in Fig. 2.

Element sizes for the full-scale wing were determined by optimizing the structure using a minimum flutter velocity constraint using a finite element-based analysis and optimization

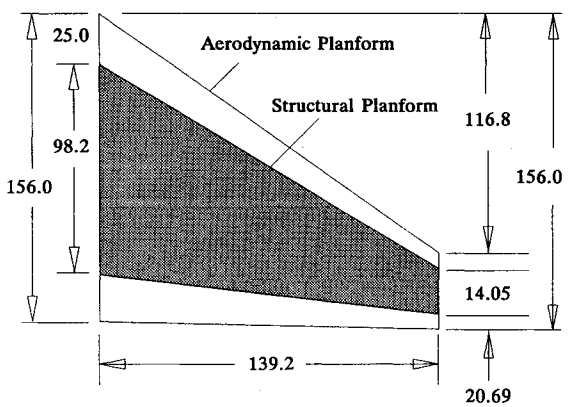

Fig. 1 Aerodynamic planform of full-scale wing.

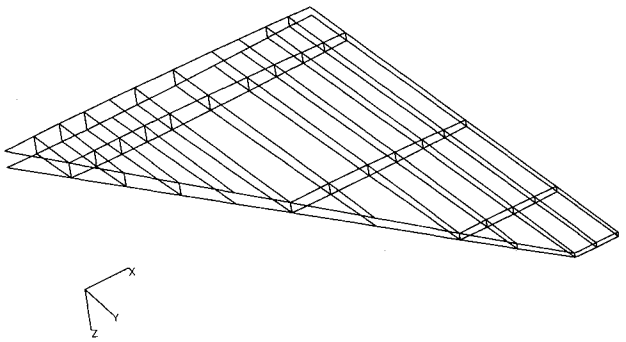

Fig. 2 Finite element representation of full-scale wing.

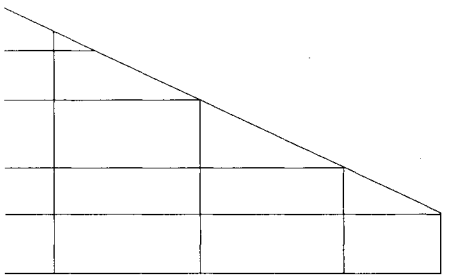

Fig. 3 Finite element representation of scale model.

package called ASTROS.[22] The minimum flutter speed was given as 833.3 ft/s (10,000 in./s) at Mach 0.80. Heavy design variable linking was used to assign five design variables for the wing. Each design variable was a constant by which the sizes of a group of elements were multiplied. ASTROS minimized the mass of the wing structure subject to the constraint that the predicted flutter velocity must be greater than 833.3 ft/s at Mach 0.80.

The nature of the analysis does not require that the predicted flutter velocity actually correspond to Mach 0.80. We performed repeated analyses on the resulting design to find a matched point, one at which the velocity corresponded to the Mach number. The matched point flutter condition was determined to be Mach 0.75 at sea level. The calculated flutter velocity was 820.5 ft/s and the flutter frequency was 5.81 Hz.

Modal participation factors for the full-scale wing at the flutter point are given in Table 1. The modal participation coefficients are simply the complex constants by which the normal modes are multiplied to form the flutter mode. The magnitudes show that the flutter mode is composed largely of the first two normal modes. We retained the first three normal modes in all flutter calculations in case the predicted flutter mechanism changed during the design.

The model scale factors were determined without a specific wind tunnel in mind. The geometric scale factor was assigned as one-tenth. The model velocity and density ratios were both assumed to be unity. Thus, we have a one-tenth scale model that will be run in a wind tunnel at Mach 0.75 at sea level. The scale factors are summarized in Table 2.

There is no requirement that grid point locations or element connectivities of the scaled model structure correspond to those of the full-scale one. For simplicity, however, we used a subset of the grid points from the full-scale structure scaled down by a factor of 10 to define the grid point for the model finite element discretization shown in Fig. 3.

Selected out-of-plane displacements from four columns of the flexibility matrix were used for the stiffness design. The first three natural frequencies and a subset of out of plane displacements from the first three mode shapes were used for the mass design. We used widths of the beam elements as design variables for the stiffness design and the masses of small tuning weights as design variables for the mass design.

Table 1 Modal participation factors for full-scale wing

Mode	Real	Imaginary	Magnitude	Phase, deg
1	0.9764	0.00	0.9764	0.0
2	0.2075	−0.0494	0.2132	−13.4
3	−0.0173	0.0309	0.0354	119.2
4	0.0040	0.00002	0.0040	0.28

Table 2 Model scale factors

Length	1/10
Stiffness	1/10
Frequency	10
Mass	1/1000

The first stiffness design resulted in some element sizes that were too small to be manufactured. Those element heights were reduced so that the moment of inertia in bending was unchanged and the width was not less than 0.050 in. The modified design was then used as an initial design for another optimization run. This process was repeated once more so that all elements were of sizes that could be easily manufactured.

ADS allows for side constraints on an optimization problem. While such constraints could be used to ensure all elements are large enough to meet manufacturing requirements, doing so would decrease the size of the feasible region in design space. We chose to retain as large a feasible region as possible at the cost of some repeated calculations. This choice is certainly open to any designer using this method.

Model Fabrication

After the design for the one-tenth scale model structure was completed a test specimen was manufactured. We did this to verify that assumptions made during the design process were valid. Our principal concern was excess material at the element joints. The excess material added mass at the joints that was not accounted for in the finite element model and increased the stiffness in the joint area.

Also, a slight change was made to the design to make the manufacturing process simpler. The math model was symmetric about the midplane of the wing. This meant that there would have been steps on each side of the structure. The actual structure was machined flat on one side and stepped on the other, making it much easier to manufacture. We assumed that resulting stiffness changes would be small. This was not borne out in testing, however, and offsets had to be included in the finite element model.

Testing Techniques

All testing was done using laser metrology. Static testing was performed by applying either a known loading or a known displacement at selected grid points on the structure and making a double exposure hologram that showed formed fringe patterns on the image of the structure representing the deformations. Quantitative data were obtained by scanning the hologram into a personal computer based image processing system. Fringe lines were marked and counted automatically and the resulting data stored for plotting.

Some static testing was performed using electronic speckle pattern interferometry (ESPI). ESPI is similar to the photographic process except that it uses a video camera in place of a photographic slide and the fringe pattern is formed electronically. The result is a two-dimensional image of the model with superimposed fringes that are lines of constant out-of-plane deformation. A single image presents the deformations over the entire model. Furthermore, the system is sensitive to deformations of as little as 0.00001 in.

Modal testing was performed using the photographic system, the video system, and a laser vibrometer. The vibrometer was used for finding the natural frequencies of the structure so that an image showing fringe lines associated with the mode shapes could be obtained.

Static Test Results

We performed two sets of static tests. The first set was from tests where a displacement was applied to the various points on the structure using a probe mounted on a fine thread micrometer. Fringe lines along the spars were counted using the image processing software and the results normalized. Since the force was not known, good agreement between test and analysis indicated correlation to within a constant multiplier.

The second set of static test results was obtained by applying a known load to the structure and absolute displacements were measured at the various grid points on the wing. It quickly became apparent that the stiffness of the test article was significantly higher than that predicted by the finite element model. Including offsets in the finite element representation improved the agreement.

Modal Test Results

Two sets of modal tests were performed, one before the mass balancing weights were added and one after. The first three natural frequencies of the structure before mass balancing are presented in Table 3. The measured and calculated natural frequencies after the addition of the tuning masses are shown in Table 4. Agreement between experiment and analysis is good, with differences being limited to a few percent in most cases. Note that the agreement is better before the tuning masses were added. Since the objective function for the mass design was not zero, an additional error is introduced when the tuning masses are added.

Obviously, the most important measure of the quality of an aeroelastically scaled model is the degree to which it reproduces the desired aeroelastic phenomena. The full scale wing has a predicted flutter instability at 820.5 ft/s at a Mach number of 0.75. The calculated flutter frequency was 5.81 Hz.

The aeroelastically scaled model has a predicted flutter speed of 759.1 ft/s and frequency of 58.1 Hz at Mach 0.75. The factor of 10 difference in the flutter frequency is due to the frequency scale factor from Table 2. The predicted modal participation factors for the model are presented in Table 5.

Table 3 Natural frequencies before mass balancing

Mode	Experimental frequency, Hz	Predicted frequency, Hz	Mode type
1	77.0	79.6	First bending
2	227.9	226.6	Second bending
3	262.2	261.9	First torsion

Table 4 Natural frequencies after mass balancing

Mode	Experimental frequency, Hz	Predicted frequency, Hz	Mode shape
1	39.5	37.9	First bending
2	127.3	118.7	Second bending
3	164.9	150.0	First torsion

Table 5 Modal participation factors for aeroelastically scaled model

Mode	Real	Imaginary	Magnitude	Phase, deg
1	0.9799	0.00	0.9799	0.0
2	0.1907	−0.0437	0.1956	−12.91
3	−0.0097	0.0382	0.0394	104.3

They compare well with the full-scale factors from Table 1, indicating that the flutter mechanism has been well modeled.

Flutter is a phenomenon made up of dynamic structural response and unsteady aerodynamic forces. For a model to accurately reproduce the flutter mechanism, both components must be reproduced accurately. The method described here results in a model structure that accurately reproduces the structural response. The flutter analysis of the completed model design assumes that the aerodynamic forces are accurately reproduced. Thus, the predicted flutter point may be closer to the desired one than the structural response alone might suggest.

Conclusions

Numerical and experimental results from this work indicate that a workable method of wind-tunnel model design has been developed. The methods presented here are easily implemented and can result in relatively simple structures that accurately meet the mass and stiffness requirements. The example problem showed that scaled flutter velocity and frequency requirements can be satisfied and that the predicted flutter mechanism is correct as well.

The method described is applicable for any structure that can be accurately modeled using a finite element discretization. The beam lattice structure used here is only an example.

Acknowledgment

The authors wish to thank Gene Maddux for his invaluable assistance in the experimental work described here.

References

[1]Felt, L., "The Graybeard Pitch," Flight Dynamics Directorate, Wright–Patterson AFB, OH, July 1993.

[2]French, R. M., "An Application of Structural Optimization in Wind Tunnel Model Design," AIAA Paper 90-0956, April 1990.

[3]French, R. M., and Kolonay, R. M., "An Application of Compound Scaling to Aeroelastic Model Design," Third Air Force/NASA Symposium on Recent Advances in Multidisciplinary Analysis and Optimization, San Francisco CA, Sept. 1990.

[4]Bisplinghoff, R. L., Ashley, H., and Halfman, R. L., *Aeroelasticity*, Addison–Wesley, Reading, MA, 1955.

[5]Ibrahim, R. S., and Saafan, A. A., "Correlation of Analysis and Test in Modeling of Structures Assessment and Review," *5th SEM International Modal Analysis Conference (IMAC)*, 1987, pp. 1651–1660, pp. 123–129.

[6]Berman, A., "System Identification of Structural Dynamic Models—Theoretical and Practical Bounds," AIAA Paper 84-0929, May 1984.

[7]Keller, C. L., "Methods for Determining Modal Parameters and Mass, Stiffness and Damping Matrices," Air Force Flight Dynamics Lab., AFFDL-TR-78-59, June 1978.

[8]Baruch, M., and Bar Itzhack, I. Y., "Optimal Weighted Orthogonalization of Measured Modes," *AIAA Journal*, Vol. 16, No. 4, 1978, pp. 346–351.

[9]Baruch, M., "Optimization Procedure to Correct Stiffness and Flexibility Matrices Using Vibration Tests," *AIAA Journal*, Vol. 16, No. 11, 1978, pp. 1208–1210.

[10]Wei, F.-S., "Stiffness Matrix Correction from Incomplete Modal Data," *AIAA Journal*, Vol. 18, No. 10, 1980, pp. 1274, 1275.

[11]Berman, A., "Mass Matrix Correction Using an Incomplete Set of Measured Modes," *AIAA Journal*, Vol. 17, No. 10, 1979, pp. 1147, 1148.

[12]Berman, A., and Nagy, E. J., "Improvement of a Large Analytical Model Using Test Data," *AIAA Journal*, Vol. 21, No. 8, 1983, pp. 1168–1173.

[13]Sidhu, J., and Ewins, D. J., "Correlation of Finite Element and Modal Test Studies of a Practical Structure," *Proceedings of the 2nd SEM International Modal Analysis Conference* (Orlando, FL), 1984, pp. 756–762.

[14]Gysin, H. P., "Critical Application of the Error Matrix Method for Localisation of Finite Element Modelling Inaccuracies," *Proceedings of the 4th SEM International Modal Analysis Conference* (Los Angeles, CA), 1986, pp. 1339–1343.

[15]Ojalvo, I. U., Ting, T., Pilon, D., and Twomey, W., "Practical Suggestions for Modifying Math Models to Correlate with Actual Modal Test Results," *Proceedings of the 7th SEM International Modal Analysis Conference* (Las Vegas, NV), 1989, pp. 347–354.

[16]Wei, M. L., and Janter, T., "Optimization of Mathematical Models via Selected Physical Parameters," *Proceedings of the 6th SEM International Modal Analysis Conference* (Kissimmee, FL), 1988, pp. 73–79.

[17]Ewing, M. S., and Venkayya, V. B., "Structural Identification Using Mathematical Optimization Techniques," *Proceedings of the AIAA 32nd Structures, Structural Dynamics, and Materials Conference* (Baltimore, MD), AIAA, Washington, DC, 1991, pp. 840–845 (AIAA Paper 91-1135).

[18]Ewing, M. S., and Kolonay, R. M., "Dynamic Structural Model Modification Using Mathematical Optimization Techniques," *Proceedings of the Computer Aided Optimum Design of Structures 91* (Boston, MA), 1991, pp. 285–295.

[19]Gibson, W. C., "ASTROS-ID: Software for System Identification Using Mathematical Programming," Wright Lab., WL-TR-92-3100, Sept. 1992.

[20]Vanderplaats, G. N., "ADS—A FORTRAN Program for Automated Design Synthesis," NASA CR 172460, Oct 1984.

[21]Venkayya, V. B., Tischler, V. A., Kolonay, R. M., and Canfield, R. A., "A Generalized Optimality Criteria for Mathematical Optimization," AIAA Paper 90-1192, April 1990.

[22]Johnson, E. H., and Venkayya, V. B., "Automated Structural Optimization System (ASTROS), Volume I—Theoretical Manual," Air Force Wright Aeronautical Labs., AFWAL-TR-88-3028, Dec. 1988.